

# Dynamics of in-plane charge separation front in 2D electron-hole gas

Gang Chen, Ronen Rapaport, Steven H. Simon, Loren Pfeiffer, and Ken West

*Bell Laboratories, Lucent Technologies,  
600 Mountain Avenue, Murray Hill, New Jersey 07974*

## Abstract

We show both experimentally and theoretically that the recently observed optically induced in-plane charge separation in quantum well (QW) structures and the exciton ring emission pattern at this charge separation boundary have an extremely long lifetime. The oppositely charged carriers remain separated and provide a reservoir of excitons at their boundary with a persistent emission which lasts hundreds of microseconds (orders of magnitude longer than their recombination time) after the external excitation is removed. This long lifetime is due to an interplay between the slow in-plane carrier diffusion and slow carrier tunnelling perpendicular to the QW plane.

Triggered by the quest for excitonic Bose-Einstein condensation (BEC), recent studies on the emission from both double and single GaAs based quantum well (QW) structures under tightly focused optical excitation revealed a surprising ring pattern which extends to a large distance away from the excitation spot<sup>1,2</sup>. It was later found that an optically induced in-plane separation of oppositely charged plasmas is responsible for this excitonic ring emission pattern formation<sup>3,4</sup>. The emerging physical picture is as follows. Since the structures are n-doped and in most experiments biased, there is an equilibrium density of 2D electron gas in the entire quantum well even in the absence of optical excitation. The external optical excitation creates hot electrons and holes above the barrier energy, some of which drift across the QW to the contacts driven by the electrical field applied perpendicular to the QW plane. The rest of the hot electrons and holes cool down into the QW. However, this cooling process is more likely for the holes due to their smaller drift velocity (by a factor of 10-20<sup>5</sup>) and shorter phonon scattering time<sup>6</sup>. This leads to a depletion of electrons that originally dwell in the QW near the laser excitation spot via fast electron-hole recombination. While the tunnelling of electrons into the QW tries to bring the electron density back to the equilibrium level, high enough optical excitation intensity will completely deplete the electrons and eventually build up an excess population of holes at the excitation spot, resulting in a hole puddle surrounded by a sea of electrons outside the excitation spot in the plane of the QW (perpendicular to the growth direction). Diffusion combined with the Coulomb repulsion<sup>7</sup> of like charges drives the holes in the puddle, and therefore the electron depletion region, outwards. In the steady state, the densities of both electron and hole plasmas at their boundary are low enough to allow for the formation of excitons. The recombination of these excitons gives rise to the large diameter ring pattern. It is important to note that this is a different phenomenon from the related giant ambipolar drift of spatially separated electrons and holes in n-i-p-i superlattice structures<sup>8,9</sup> (see endnote<sup>10</sup> for more explanation).

The above picture portrays an interesting interplay of various physical processes, such as carrier tunnelling (across the QW), diffusion, drift (in the QW plane), and optical recombination. These processes have distinct time scales and their interplay directly determines the dynamics of the in-plane charge separation and ring emission pattern. In this paper, we explore this dynamics by measuring the response of the charge separation front to abrupt changes in optical excitation intensity at the center spot. We found that the overall reaction

of the charge separation is surprisingly slow: it takes the ring emission pattern hundreds of microseconds to expand outward to the steady-state position after turning on the optical excitation and hundreds of microseconds to collapse into the center spot after turning off the excitation. Theoretical analysis show that this extremely long lifetime is a result of the slow carrier diffusion in the QW and tunnelling across the QW. This extremely persistent charge separation also provides an exciton reservoir that lasts orders of magnitude longer than the exciton lifetime. In addition, since the optically generated excess holes spend such a long time to diffuse to the ring, they may have been well thermalized to the lattice temperature before the formation of excitons.

As in our previous work<sup>3</sup>, the sample consists of a single 60Å In<sub>0.13</sub>Ga<sub>0.87</sub>As quantum well surrounded by GaAs/Al<sub>0.32</sub>Ga<sub>0.68</sub>As 50Å/1000Å barriers. A 1000 Å layer of Si doped GaAs is located 2000 Å from the QW on the  $n^+$  substrate side and another similar layer is located 1000Å from the QW on the top contact side. Gold films are deposited on both sides of the sample to form contacts. A 1 mm hole is opened on the top gold film for the optical measurements. The sample was measured at 6K, and excited with a HeNe laser (632 nm) with a spot diameter of  $\sim 60\mu m$ .

In the particular experiments to be discussed below, the excitation power ( $I$ ) at the center was modulated, with a modulation period  $T$ , between two values ( $I_h = 900\mu W$  and  $I_l = 800\mu W$ , square modulation), and with a fixed applied bias voltage across the sample. The ring emission was imaged onto a liquid nitrogen cooled CCD camera. Each image was collected over an exposure time much longer than  $T$ . Figure. 1 (a)-(b) show examples of collected images. Figure. 2(a) shows the square light intensity modulation profile. At a modulation period of  $T=10$  ms (Fig. 1(a)), two sharp concentric rings are clearly observed with no emission in between. As  $T$  is decreased (faster modulation), the emission intensity in the region *between* the two original rings grows until the two concentric rings transform into a wide emission annulus, as can be seen in Fig. 1(b) for  $T=0.33$ ms. This can be simply explained as follows. For a very slow modulation, the transit time  $t_0$  for the charge separation front (observed as the ring emission) to move from one steady state position to the other corresponding to the two excitation intensities  $I_h$  and  $I_l$  is much smaller than  $T/2$ . Therefore, one expects that the emission ring will spend most of the time in the two steady state positions. Since the image is integrated over many modulation cycles, most of the light is expected to be emitted from two concentric rings. As  $T$  decreases, the charge separation

front spends relatively more time in transit, leading to an increased emission from the region in between the two steady state positions and therefore a decreased contrast of the rings relative to the plateau in between. When  $t_0 \approx T/2$ , the charge separation front spends all of its time in transit ( $t_0$  going outward and another  $t_0$  going inward), which diminishes the contrast of the rings and gives rise to an annulus emission pattern. Experimentally, such transition occurs around  $T \sim 300 - 500 \mu s$  (a modulation frequency of 3-2KHz, depending on the applied bias), implying a surprisingly long transit time  $t_0$ , on the order of hundreds of microseconds.

In a different experiment, the excitation intensity was fixed while the applied bias was modulated between two values (similar square wave modulation). The emission images are similar to those taken in the light intensity modulation experiments. Again, a transition from two concentric rings to a flat annulus at a modulation period of hundreds of microseconds was observed. While the excitation intensity modulation changes the carrier density locally around the center excitation spot, the bias voltage modulation changes several parameters across the entire sample, including the carrier tunnelling time and the branching ratio of the optically generated hot electrons and holes above the barriers cooling into the QW. Therefore, the analysis of the light modulation experiments are more straightforward.

Examples of the emission profiles showing the transition from two concentric rings to a flat annulus are plotted in Fig. 1(c) and Fig. 1(d) for the excitation intensity and bias voltage modulation experiments, respectively. We further define a measurable quantity, the contrast of the concentric ring relative to the annulus, as  $C = \frac{I_2}{I_1}$ , where  $I_1$  is the *average* peak emission intensity of the two rings, and  $I_2$  is the difference between  $I_1$  and the emission intensity of the plateau *midway* between the rings, as illustrated in the middle curves of Fig. 1(c)-1(d).  $C$  clearly depends on both the modulation frequency and the ring response time  $t_0$ . Based on previous discussions,  $C$  should approach unit (maximum contrast) at low modulation frequency and decrease as the modulation frequency increase.

To show how  $C$  should look in a simple way, we first assume that the charge boundary moves at a constant speed between the two steady state positions (we will show later why this assumption is justified), spending a time of  $t_0$  going outward and an identical amount of time  $t_0$  going inward in each modulation cycle. This is shown by the thin dark solid line in Fig. 2(b). On average, the charge boundary spends  $2t_0$  in each modulation cycle in transit and the rest of the time at the two steady state positions. For such a response integrated

much longer than  $T$ , the contrast  $C$  should take the form of  $C = \frac{T/2-t_0}{T/2-t_0+2At_0}$  for  $T \geq 2t_0$ , where  $A$  is the ratio of the ring spatial width and the width of the annulus. As expected, the contrast  $C$  varies between 1 (two concentric rings) and 0 (a flat annulus) as  $T$  goes from infinity to  $2t_0$ . For  $T < 2t_0$ , the contrast should stay zero (flat annulus).

The measured contrast  $C$  for the light and bias voltage modulation experiments is plotted in Fig. 3(a) and Fig. 3(b), respectively. The solid line in Fig. 3(a) shows the fitted  $C$  for the light modulation experiments with  $A = 0.25$  (obtained by measuring the width of the annulus and the rings). The fitting yields a  $t_0$  of 260  $\mu s$ . For the voltage modulation experiments,  $A$  is  $\sim 0.4$  and the fitted solid line in Fig. 3(b) gives a  $t_0$  of 250  $\mu s$ .

For  $T < 2t_0$ , the emission pattern remains a flat annulus. However, since the charge separation front does not have enough time to move the full range between the two steady state positions for fast modulation, the annulus should narrow with decreasing  $T$ . As an example, the annulus width,  $w$ , as a function of the modulation frequency for the same set of bias modulation experiments in Fig. 3b is plotted in Fig. 3c. A simple calculation, again assuming that the ring moves in and out at a constant speed, shows that the dependence of  $w$  on  $T$  is of the form  $w = w_0 \frac{T}{2t_0}$ , where  $w_0$  is the radial distance between the two rings at low modulation frequencies. We use the value for  $t_0$  obtained from Fig. 3(b) and plot  $w$  as a solid line in Fig. 3(c). It fits the data points very well.

We now discuss how this extremely long response time comes about based on the model presented earlier and in Ref.<sup>3,4</sup>. Generally speaking, the charge separation boundary responds to the change of excitation intensity on a time scale determined by both the carrier diffusion and drift time in the QW plane and the tunnelling time through the QW. Details of this dependence will be discussed later. In Fig. 2(b), the thick gray line shows the numerically calculated ring emission response (using Eq. 1-2 described below) for a carrier tunnelling time of 50  $\mu s$  and an electron and hole diffusion coefficient of 20  $\mu m^2/ns$  and 2  $\mu m^2/ns$ , respectively. The excitation light is modulated between 800 and 900  $\mu W$  with a periodicity of  $T=400 \mu s$ . The calculation clearly shows that the ring response time is indeed extremely long. In addition, the ring does not expand and contract at a constant speed: it moves faster right after the abrupt change of excitation intensity and then gradually slow down. However, at a particular ring position, the expansion and contraction speeds roughly compensate such that the average speed for every ring position during each modulation cycle almost does not change. This justifies the earlier assumption that for images integrated

much longer than  $T$  the charge separation boundary looks as if it moves at a constant speed between the two steady-state positions.

It is important to note that the above experiments were also performed under different excitation intensity modulation depth. We found that the ring response time does not vary much even for modulations in which  $I_l$  is almost zero and the charge boundary moves all the way between the excitation spot and a large diameter ring. These observations are consistent with the numerical calculations.

We now discuss how  $t_0$  depends on the carrier diffusion and tunnelling times by analyzing the response of the cold electron and hole densities ( $n$  and  $p$ ) in the QW determined by two coupled rate equations<sup>3,4,7</sup> (neglecting the Coulomb repulsion of like charges, which does not greatly alter the numerical results qualitatively<sup>7</sup>):

$$\frac{\partial n}{\partial t} = D_n \nabla^2 n - \frac{n - n_{eq}}{\tau_e} - \xi n p + f_n \quad (1)$$

$$\frac{\partial p}{\partial t} = D_p \nabla^2 p - \frac{p}{\tau_h} - \xi n p + f_p \quad (2)$$

Here,  $D_e$  and  $D_h$  are the electron and hole in-plane diffusion-drift coefficients;  $\tau_e$  and  $\tau_h$  are the electron and hole leakage (tunnelling) times;  $f_n$  and  $f_p$  are the cold electron and hole sources due to the cooling of optically generated hot carriers into the quantum well;  $n_{eq}$  is the constant equilibrium density of electrons in the QW in the absence of the optical excitation; and  $\xi$  is the electron-hole capture coefficient. To simplify further analysis, we assume that  $D_e = D_h \equiv D$  and  $\tau_n = \tau_h \equiv \tau$ . The charge imbalance  $z = p - n$  then satisfies

$$\frac{\partial z}{\partial t} = D \nabla^2 z - \frac{z - z_0}{\tau} + f_z \quad (3)$$

where the original charge imbalance  $z_0 = -n_{eq}$  and  $f_z = f_p - f_n$  is the charge imbalance source. It is important to note that the exciton ring appears at the contour of  $z = 0$  (the boundary between the electrons and holes).

The stationary solution of Eq. 3 is shown by the gray solid line in Fig. 4(a) for a time *independent* excitation source at a small excitation spot with a Gaussian profile (60  $\mu\text{m}$  full width half maximum). The charge imbalance response dynamics can then be obtained by solving Eq. 3 using this stationary profile as the initial condition and turning off the optical excitation ( $f = 0$ ). This corresponds to our light modulation experiments with a large modulation depth. If we now approximate this initial stationary charge imbalance distribution as a Gaussian function  $z(r, t=0) = M e^{-\frac{r^2}{\Delta^2}} - n_{eq}$  which has an identical peak value

and an integrated value above  $n_{eq}$  (the dashed Gaussian line in Fig. 4(a); the validity of this approximation will be discussed later), the solution of Eq. 3 becomes

$$z = n_{eq} \left( \frac{t_D}{t + \Delta^2/4D} e^{\frac{-r^2}{4Dt + \Delta^2}} e^{-\frac{t}{\tau}} - 1 \right), \quad (4)$$

where the diffusion characteristic time is given by  $t_D = M\Delta^2/4Dn_{eq}$ .

Figure. 4(b) shows this charge imbalance profile at two different times. At  $t=0$ , it starts as a Gaussian and the position of the emission ring is determined by  $z = 0$  (marked by the arrows in Fig. 4(b)). It then broadens and decreases in amplitude. At  $t = t_0$ , where  $t_0$  is the ring response time discussed in the experiments, the charge imbalance peak shrinks to just below  $z = 0$  and the ring collapses to the center spot.  $t_0$  satisfies  $z(r = 0, t = t_0) = 0$ , or  $t_0 + t_D n_{eq}/M = t_D e^{-t_0/\tau}$ , and is plotted in Fig. 4(c) as a function of  $\tau$  in units of  $t_D$ . We see that the ring response is determined by both the diffusion time  $t_D$  and the tunnelling time  $\tau$ . In particular, it shows that  $t_0$  is upper-bounded by  $t_D(1 - n_{eq}/M)$  for large  $\tau$ . As  $\tau$  becomes shorter,  $t_0$  decreases and is eventually determined by  $\tau$  for  $\tau \ll t_D$ . Note that  $M$  is the amplitude of the initial charge imbalance. It is obvious that  $M > n_{eq}$  (complete electron depletion at the excitation spot) is a necessary condition for the ring formation and a positive  $t_0$ .

The experimental peak carrier imbalance density at the excitation spot is roughly  $M = 2 \times 10^{12} \text{cm}^{-2}$ , which is extracted from the measured linewidth of the emission<sup>3</sup>. The equilibrium carrier imbalance density  $z_0$  is extracted to be  $10^{11} \text{cm}^{-2}$  by measuring the linewidth of the emission at very low excitation intensity. The characteristic diffusion time,  $t_D$ , is then calculated to be  $250 \mu\text{s}$  for a hole diffusion coefficient of  $2 \mu\text{m}^2/\text{ns}$  and  $\Delta = 300 \mu\text{m}$  (estimated from an outer ring radius of  $400 \mu\text{m}$ ). Assuming that the tunnelling time is much larger than  $t_D$ ,  $t_0$  is then  $\sim t_D(1 - n_{eq}/M) = 225 \mu\text{s}$ . This is in good agreement with the experimentally measured value, particularly considering various approximations we have made.

The above analytical solution of the ring response is based on the assumption that the steady-state charge imbalance profile is a Gaussian. The validity of this approximation is verified by the identical  $t_0$  numerically determined using either the numerically simulated steady-state charge imbalanced profile or its Gaussian approximation (Fig.4(a)) as the initial condition.

An important implication of the extremely long response time is that after the excess holes are generated at the excitation spot, they spend hundreds of microseconds migrating to

where the emission ring is. Therefore, it is expected that these initially hot holes generated optically in the QW should have enough time to thermalize to the lattice temperature. Compared to directly and nonresonantly generated hot excitons, the excitons formed at the ring should have a kinetic energy that is no more than the exciton binding energy. In addition, the supply of the excitons at the ring is extremely persistent: the positive and negative charge plasmas remain separated with excitons formed at their boundary for microseconds even after the optical excitation source is turned off.

We thank Phil Platzman, David Snoke, and Xing Wei for helpful discussions.



- 
- <sup>1</sup> D. Snoke, S. Denev, Y. Liu, L. Pfeiffer, and K. West, *Nature* **418**, 754 (2002).
- <sup>2</sup> L. V. Butov, A. C. Gossard, and D. S. Chemla, *Nature* **418**, 751 (2002).
- <sup>3</sup> R. Rapaport, G. Chen, D. Snoke, S. H. Simon, L. Pfeiffer, K. West, Y. Liu, and S. Denev, *Phys. Rev. Lett.* **92**, 117405 (2004), condmat/0308150 (2003).
- <sup>4</sup> L. V. Butov, L. S. Levitov, A. V. Mintsev, B. D. Simons, A. C. Gossard, and D. S. Chemla, *Phys. Rev. Lett.* **92**, 117404 (2004).
- <sup>5</sup> S. Adachi, ed., *Properties of Aluminum Gallium Arsenide* (INSPEC, the Institute of Electrical Engineers, London UK, 1993), ISBN 0 85296 558 3.
- <sup>6</sup> J. Shah, *Hot Carriers in Semiconductor nanostructures: Physics and Applications* (Academic Press, New York, 1992), ISBN 0-12-638140-2.
- <sup>7</sup> D. Snoke, S. Denev, Y. Liu, S. H. Simon, R. Rapaport, G. Chen, L. Pfeiffer, and K. West, condmat/0406141 (2004).
- <sup>8</sup> K. H. Gulden, H. Lin, P. Kiesel, P. Riel, G. H. Dohler, and K. J. Ebeling, *Phys. Rev. Lett.* **66**, 373 (1991).
- <sup>9</sup> M. Beck, D. Streb, M. Vitzethum, P. Kiesel, S. Malzer, C. Metzner, and G. H. Dohler, *Phys. Rev. B* **64**, 085307 (2001).
- <sup>10</sup> In the n-i-p-i superlattice structures, the electrons and holes are separated along the growth direction driven by the built-in electric field. The enhanced diffusion coefficient and the negligible optical recombination (due to the electron-hole separation) are both critical to the giant carrier diffusion. In the QW structures, however, the electrons and holes are confined in the same QW and separated in-plane. A fast optical recombination is crucial for the electron depletion, the large charge separation, and the emission ring formation.

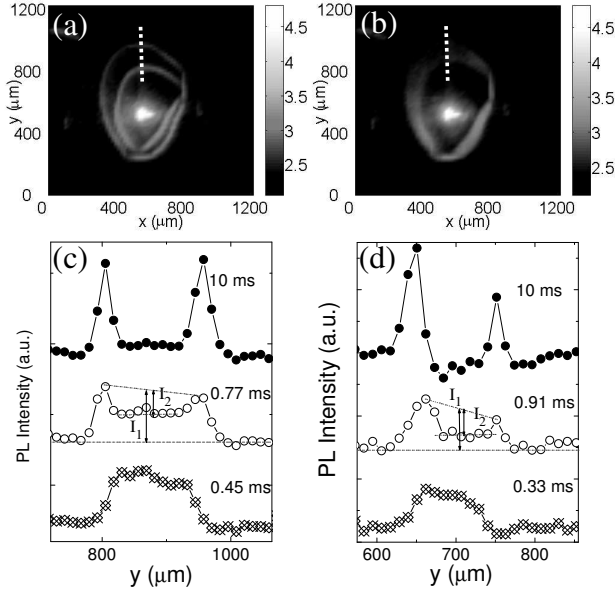


FIG. 1: PL images for light intensity modulation experiments at a modulation period of (a) 10 and (b) 0.33 ms (0.1 and 3 KHz). (c) Emission profile along the dashed line in (a) and (b) for various modulation periods, showing the transition from two concentric rings to an annulus. (d) is similar to (c), except that the bias voltage instead of the light intensity is modulated. The schematics in the middle curves of (c) and (d) show how the ring contrast,  $C = \frac{I_2}{I_1}$ , is defined.

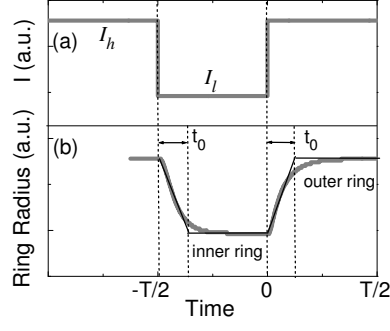


FIG. 2: (a) A schematic for the square modulation of the optical excitation intensity between two values  $I_h$  and  $I_l$ . (b) The thick gray and thin dark lines describe the numerically calculated and simplified charge separation boundary (ring) response within one modulation cycle. It spends  $t_0$  moving inward, another  $t_0$  moving outward, and the rest of the time at the two steady-state positions.

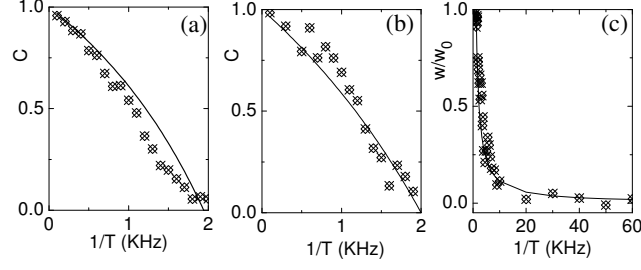


FIG. 3: Contrast  $C$  of the two emission rings relative to the annulus as a function of the modulation frequency for (a) the light modulation and (b) the bias voltage modulation experiments. The solid lines are fit using  $C = (T/2 - t_0)/(T/2 - t_0 + At_0)$ , where the ring response time  $t_0$  is the only fitting parameter (see the text). (c) Normalized annulus width  $w$ , as a function of modulation frequency for the bias voltage modulation experiments. The solid line represents  $w/w_0 = T/2t_0$ , where  $t_0$  is taken from the fitting in (b).

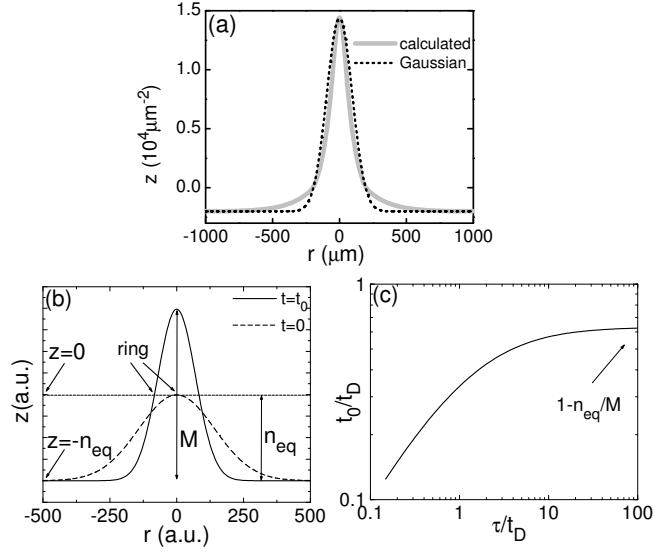


FIG. 4: (a) The solid gray line is the numerically calculated steady-state charge imbalance density profile,  $z$ , under a time-independent optical excitation (at  $r=0$ ) which has a gaussian profile with a full width half maximum of  $60 \mu\text{m}$ . The dashed line is a Gaussian with a peak value and an integrated charge imbalance above  $n_{eq}$  identical to the numerical calculation. (b) Profiles of  $z$  at  $t = 0$  and  $t = t_0$ . The optical excitation at the center spot is turned off at  $t = 0$ . The ring appears at where  $z = 0$ . The ring radius shrinks with time and at  $t_0$  it completely collapses.  $M - n_{eq}$  is the peak  $z$  at  $r = 0$  before the optical excitation is turned off and  $n_{eq}$  is the dark equilibrium electron density in the QW. (c)  $t_0$  as a function of the tunnelling time  $\tau$  in units of the characteristic diffusion time  $t_D$ .  $t_0$  is upper-bounded by  $t_D(1 - n_{eq}/M)$  for large  $\tau$  and decreases with decreasing  $\tau$ .